BBC RD 1976/25

BBC

RESEARCH DEPARTMENT

1974
THE QUEEN'S AWARD TO INDUSTRY

REPORT

A wideband Band III aerial

R.D.C. Thoday, C.Eng., M.I.E.R.E.

Research Department, Engineering Division
THE BRITISH BROADCASTING CORPORATION September 1976

BBC RD 1976/25
UDC 621.396.67.029.62

A WIDEBAND BAND II AERIAL

R.D.C. Thoday, C.Eng., M.I.E.R.E.

Summary

A wideband Band II aerial array has been designed using computer techniques. The aerial is intended for both transmitting and receiving purposes at Band II frequencies in the range 88 to 100 MHz.

Issued under the authority of

G D Monteath

Research Department, Engineering Division,
BRITISH BROADCASTING CORPORATION

Head of Research Department

September 1976

(RA-149)

A WIDEBAND BAND II AERIAL

A WIDEBAND BAND II AERIAL

R.D.C. Thoday, C.Eng., M.I.E.R.E.

1. Introduction

The number of v.h.f. radio programmes broadcast in the UK may be increased in the future. At present, the lower and mid-band frequencies of the Band II spectrum are almost fully utilised by the existing national programme network and local radio transmissions. The frequency allocation for a new network transmission would probably be fitted into the upper frequency range of Band II between 97 and 100 MHz.

The performance of some existing Band II transmitting aerials may present problems at the new frequencies. It is thought that many of the high-power aerial installations will operate satisfactorily over the increased bandwidth although the necessary adjustments to provide an acceptable input impedance may be difficult to achieve in practice. For some low-power installations, Yagi aerials have been used as the basic radiating element for the horizontally polarised transmitting arrays. The Yagi aerials have a limited bandwidth for satisfactory radiation patterns and impedance, the deterioration in performance usually being more rapid at frequencies above the design frequencies than those below it. As a result, the performance of existing Yagi aerials at the new frequencies would not be acceptable. With this fact in mind a wideband multi-element aerial has been designed, using computer techniques. In this design all elements are driven, in contrast to the single driven element in a Yagi. Scale-model measurements have been made to confirm the accuracy of the computed aerial performance.

2. Aerial requirements

The required aerial performance is based mainly on existing Yagi characteristics. Almost all of the Yagis used at present as Band II transmitting aerials are three-element arrays having individual gains ranging from 4·7-5·7 dB. It is desirable that the rear and side-lobe levels of the radiation pattern should be less than −20 dB relative to the maximum of the main lobe and should be maintained over a frequency band from 88 to 100 MHz. These figures are not achieved at all with some Yagis and for those which do, the performance is held only for a bandwidth of approximately 4%.

The input impedance should be 50Ω for transmitting aerials. The physical size of the aerial is important and three or four elements is considered acceptable.

3. Computer program

A computer program has been written which enables the performance of end-fire arrays using all driven elements to be calculated. Its main features are that it is possible

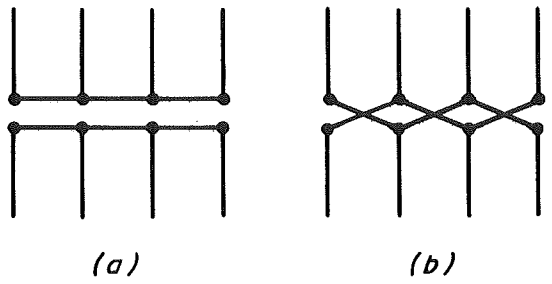

Fig. 1 - Element and interconnecting feeder arrangement

(a) Parallel
(b) Alternate

to compute the radiation patterns, gain, element currents and input impedance over a specified frequency range at specified intervals. The effect on the pattern, gain and impedance of stacking pairs of aerials can also be computed.

The program can cover either of the feeder arrangements shown in Figs. 1(a) and 1(b). The array input can be specified at the terminals of any dipole. The input data is for element length and thickness, element spacing characteristic impedance (Z_o) and length of inter-connecting feeder. A more detailed description of the program is given in Appendix 1.

4. Results of computations

The number of permutations of input parameters described in Section 2 above is large and it is both expensive and time consuming to make a really comprehensive investigation of all combinations of parameters. The design finally obtained substantially meets the requirements of Section 1.

Computations were started with three-element arrangements using both the parallel and alternate feeder system shown in Fig. 1(a) and (b). It became apparent from these early computations that the alternate feeder system provided the wider bandwidth for low rear and sidelobe levels and that the combination of three-elements would not cover the wanted bandwidth. Further calculations were made for an array of four elements. The dimensions of the array giving the best performance is shown in Fig. 2. All element diameters are 0·02m. The interconnecting feeders have the same electrical length as the element spacings. A short-circuited section of line has been added to the rear element. The length of this line influences the impedance and radiation patterns of the aerial.

4.1. Radiation patterns

The computed H- and E-plane radiation patterns for frequencies between 85—105 MHz are shown in Figs. 3(a)—(e), Fig. 4(a)—(e) respectively. The E-plane rear and sidelobe levels are less than —20 dB relative to the maximum of the main lobe over the frequency band 85 to 100 MHz.

4.2. Gain

The computed gain of the single array is shown in Fig. 5. This shows a small variation with frequency but it is comparable with the gain variation of a three-element Yagi operating over a smaller bandwidth.

4.3. Element currents

The amplitudes and phases of the element currents are shown in Fig. 6. Their values are relative to a unit current fed into the input terminals.

4.4. Input admittance

The input admittance characteristic, shown in Fig. 7 is normalised to 20mS. This, as it stands, is unsatisfactory for a transmitting aerial and a suggested method of external matching is given in Appendix II. However, as a receiving aerial, the impedance match to a 75Ω cable would, in most cases be acceptable.

5. Scale-model measurements

A small-scale model of the array was constructed using a scale factor of 1:6·3. The h.r.p. measurements were made in the frequency range 530—660 MHz. The measured plots have been included in Figs. 3(a)—(c) and 4(a)—(c). They show good agreement with the computed plots.

The input admittance of the model was measured on a network analyser, the results which have been included in Fig. 7(a) and (b) are not in full agreement with the theoretical prediction. The differences are probably a result of additional drive point capacitance and inductance which could not be easily eliminated from the model.

6. Stacked pairs of arrays

The mutual coupling between parallel arrays modifies their individual performance. For the two horizontal arrays stacked vertically, variation of back-to-front ratio with frequency, at various separations, is shown in Fig. 8. Similarly the gain variation is shown in Fig. 5. The back- and side-lobe levels increase to a maximum at a spacing of 0·75λ where the gain is also at a maximum value. An improvement in the pattern at this spacing could probably be made by further adjustment of element lengths, but the performance at spacings greater than 1λ is not seriously impaired and the loss in maximum gain is not greater than 0·3 dB.

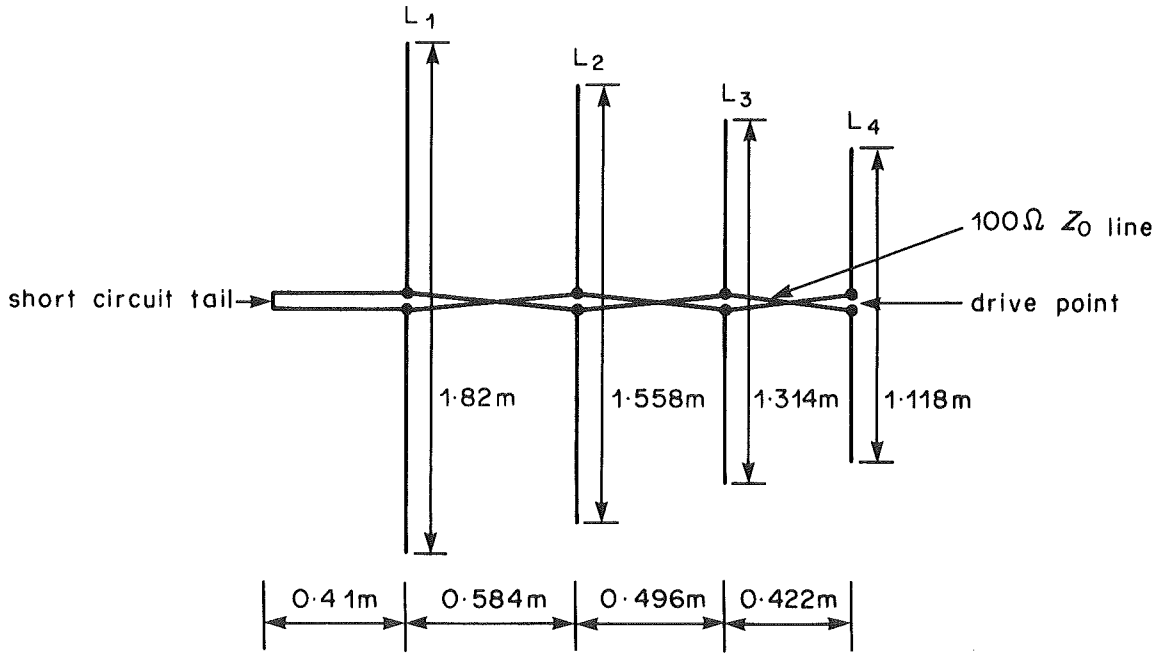

Fig. 2 - Dimensions of finalised aerial design

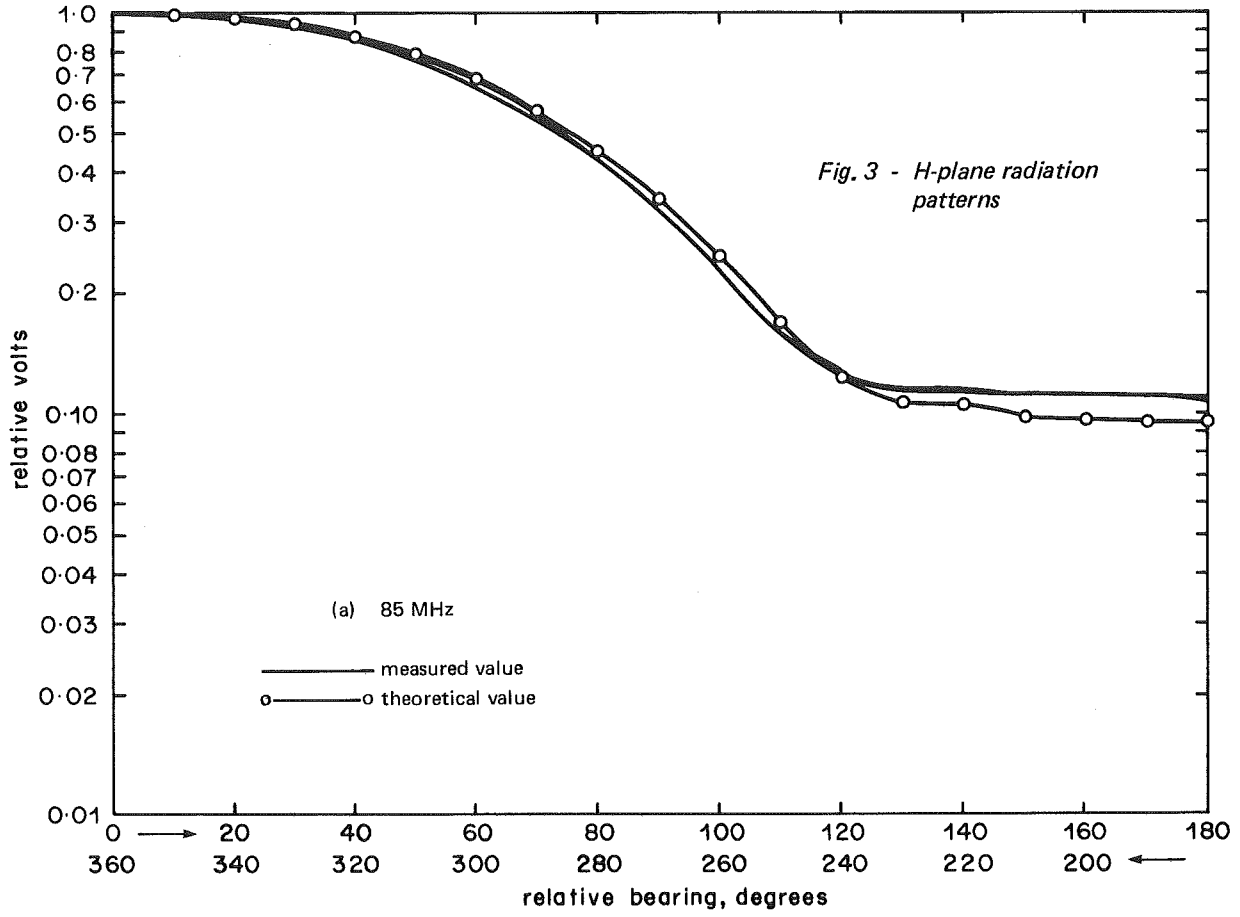

Fig. 3 - H-plane radiation patterns

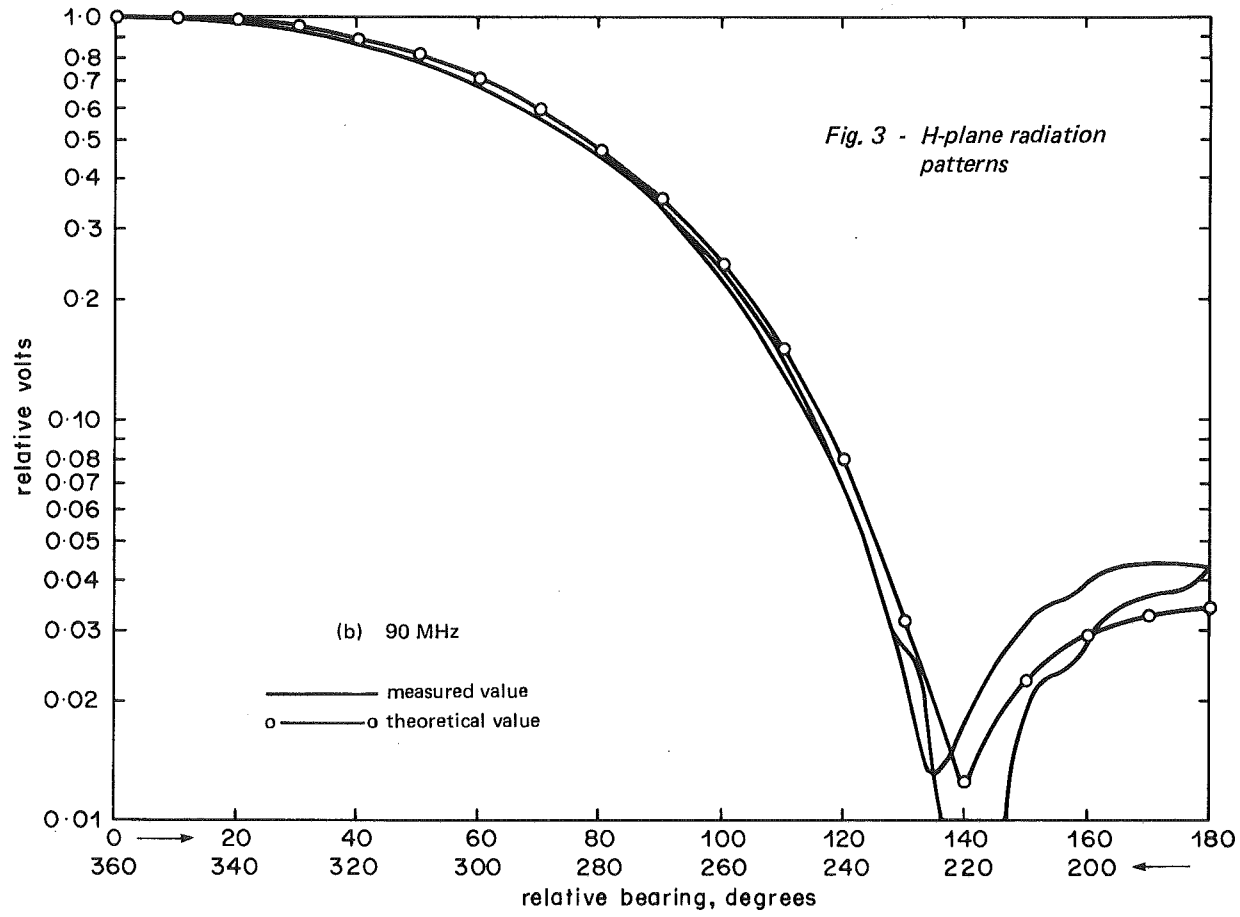

Fig. 3 - H-plane radiation patterns

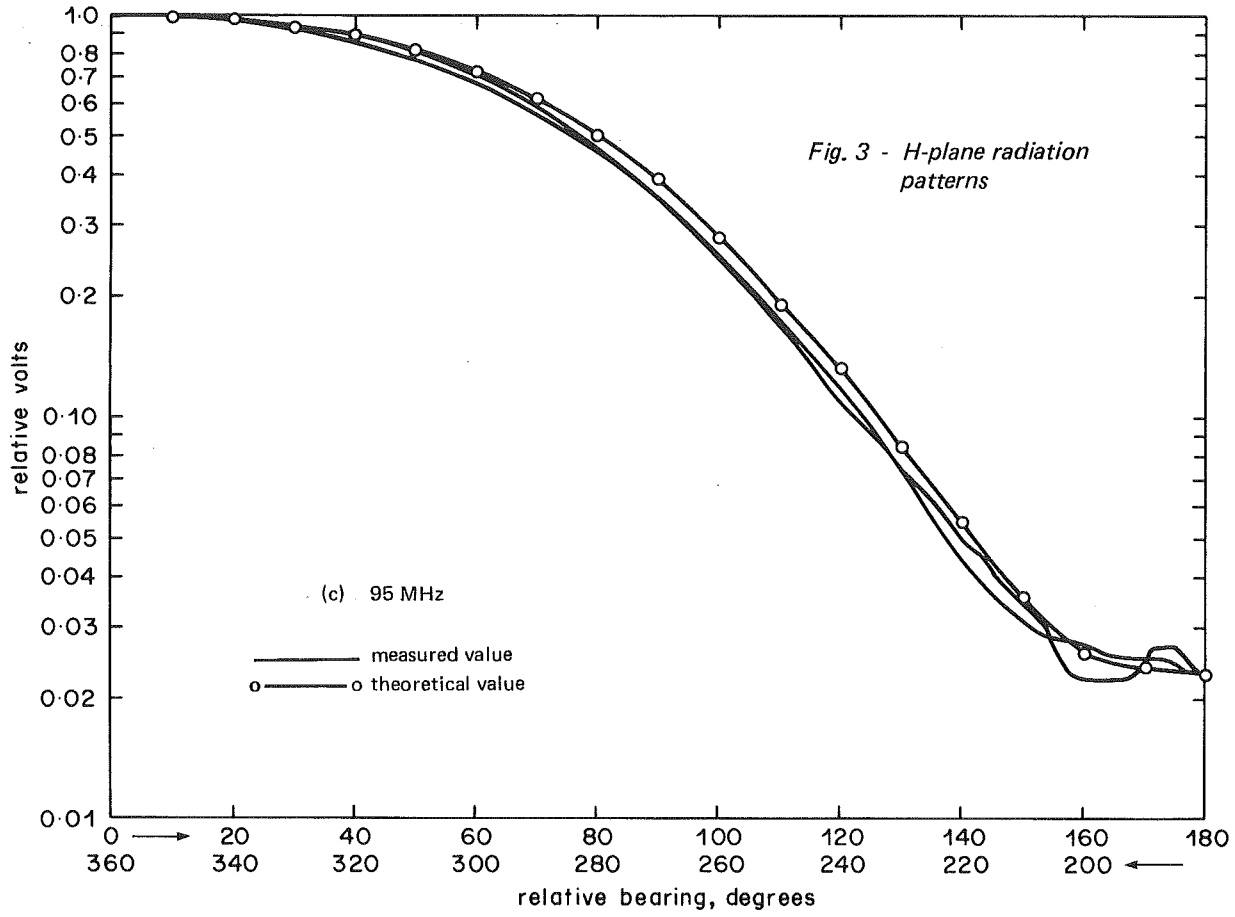

Fig. 3 - H-plane radiation patterns

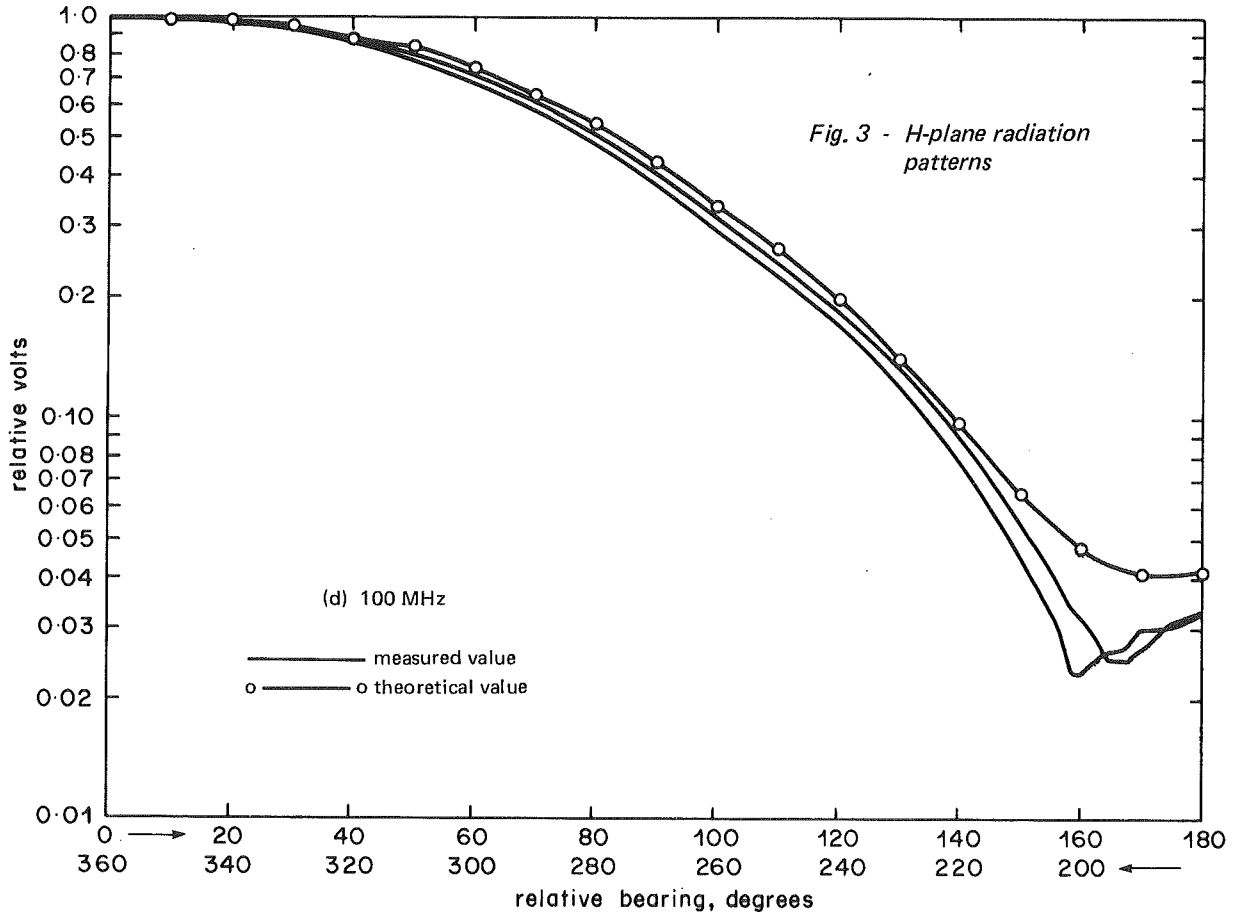

Fig. 3 - H-plane radiation patterns

using a v.h.f. admittance bridge. The input impedance of the aerial amplifier at 30 MHz is 56 – j1060Ω and that of the distribution amplifier is 8 – j295Ω. Both these measurements were made after the bias controls had been set for best linearity.

4.2. Linearity

Measurement of linearity by observing harmonic distortion is prone to error due to the levels of harmonics produced by all signal generators. Intermodulation distortion can be measured more reliably and a 'two tone test' was used to measure the linearity of the amplifiers. The arrangement used is shown in Fig. 7. The two signal generators were both capable of supplying about 5 V r.m.s. signal, therefore R2 and R1 were made large (350 and 750Ω respectively) so that cross coupling between generators was reduced. The level of intermodulation products produced by adding the signals together in this way was −120 dB below an output voltage of 0·5 V r.m.s. at the input of the amplifier.

The two signals intermodulated in the amplifier and produced intermodulation products (i.p.'s). The amplifier was followed by a band pass filter which allowed the i.p. being measured to be passed to the spectrum analyser and

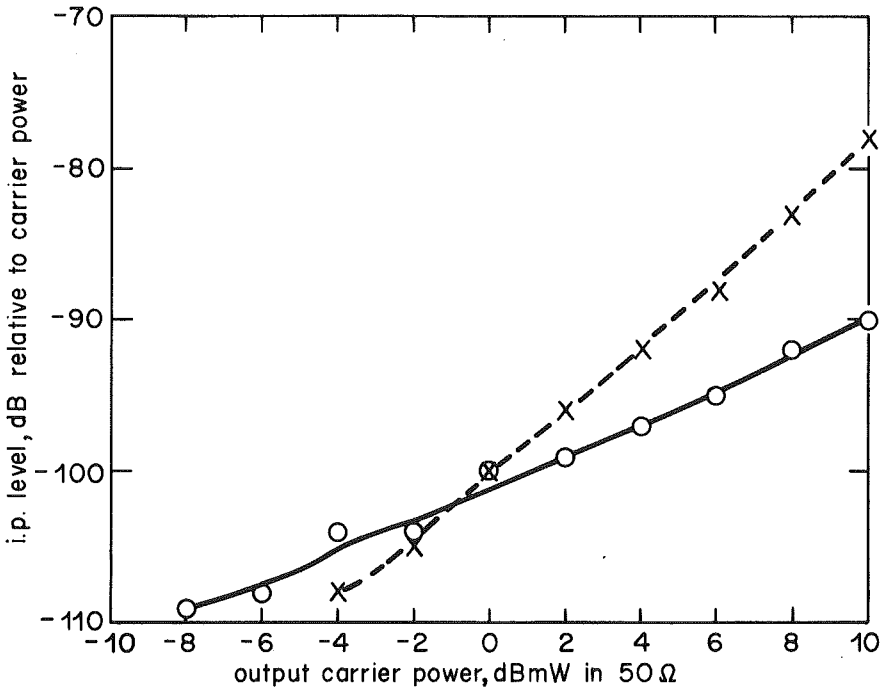

Fig. 8 - Result of two tone test on distribution amplifier

O——O 2nd order
X- - -X 3rd order

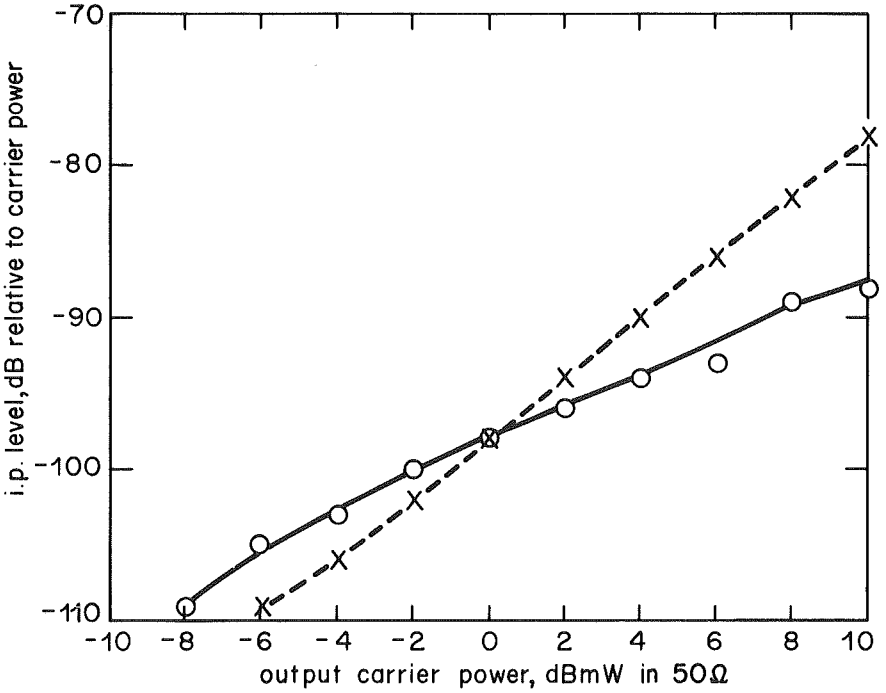

Fig. 9 - Result of two tone test on aerial amplifier

O——O 2nd order
X- - -X 3rd order

prevented intermodulation taking place in the analyser itself.

The frequencies of the two generators f_1 and f_2 were chosen so that the i.p. being measured fell within the pass-band of the filter. Measurement was confined to second-order ($f_1 + f_2$ etc.) and third-order ($2f_1 - f_2$ etc.) i.p.s.

Figs. 8 and 9 show the results of the two tone test on the distribution and aerial amplifiers respectively. The filter used for these tests had a pass band of 150 kHz centred on 10·7 MHz. In the second order test f_1 = 6·4 MHz and f_2 = 4·3 MHz and in the third order test f_1 = 7·5 MHz and f_2 = 4·3 MHz.

4.3. Noise performance

4.3.1. Distribution amplifier

In a 50Ω system the distribution amplifier may be used with its input terminated or unterminated. Therefore the noise factor was measured from a 50Ω source with and without a terminating resistor. Both measurements were made at 20 MHz.

Noise factor unterminated = 6·5 dB
Noise factor terminated = 11 dB

4.3.2. Aerial amplifier

As explained in Section 2, the measurement of the noise in the aerial amplifier is given in terms of an output noise factor. This has to be measured with the input to the amplifier terminated in an impedance equivalent to that of the monopole at that frequency. The arrangement for this test is shown in Fig. 10.

The noise from the amplifier was measured on the detector and the level noted. The noise generator was then switched on and the noise level adjusted until it was the same as the amplifier produced. The generator was calibrated in noise power into 50Ω above thermal noise and

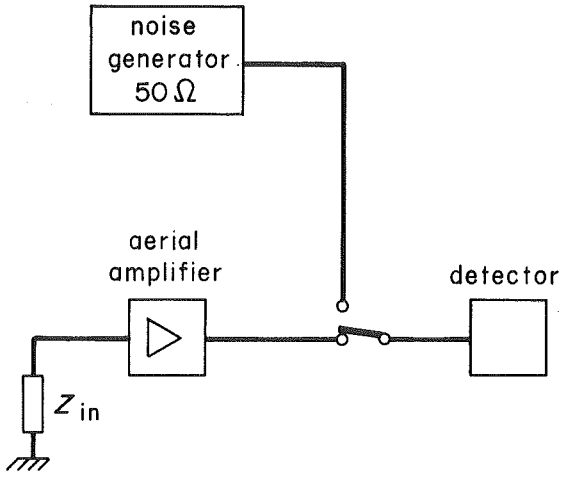

Fig. 10 - Measurement of output noise factor of aerial amplifier

therefore it was possible to determine the noise factor directly.

Fig. 11 shows how the output noise factor varies with frequency.

Table 1 shows the values of Z_{in} that were used for the test, these values are equivalent impedances to a 2m monopole at these frequencies.[3]

TABLE 1

Equivalent Z_{in} used in output noise factor test

Frequency	Impedance of 2m monopole	Component used in Z_{in}
30 MHz	20 – j100	20Ω with 56 pf
20 MHz	6 – j350	22 pf
10 MHz	1 – j700	22 pf
3 MHz	0 – j3200	16 pf

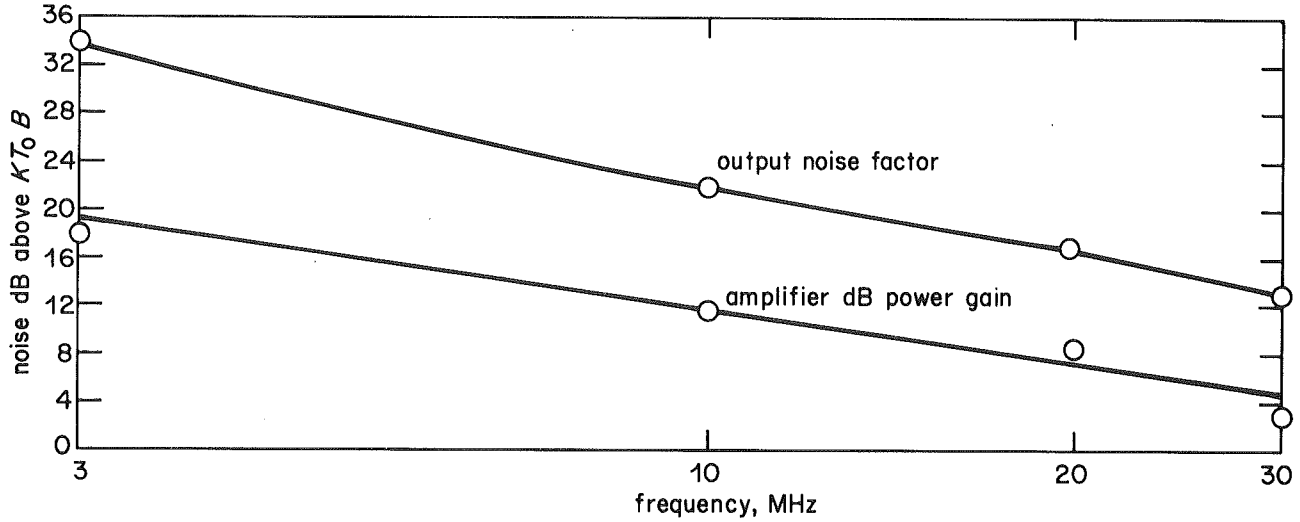

Fig. 11 - Output noise factor v's frequency

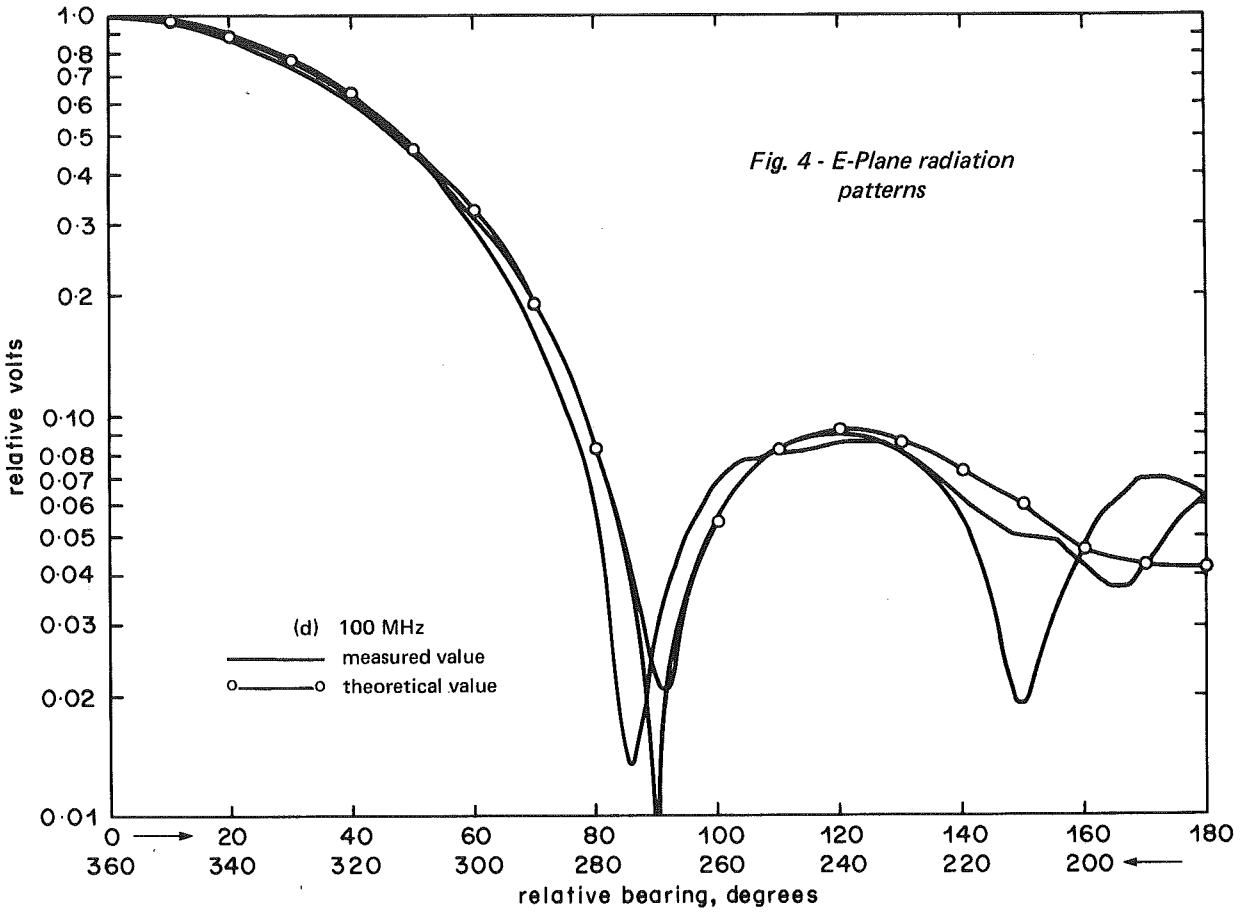

Fig. 4 - E-Plane radiation patterns

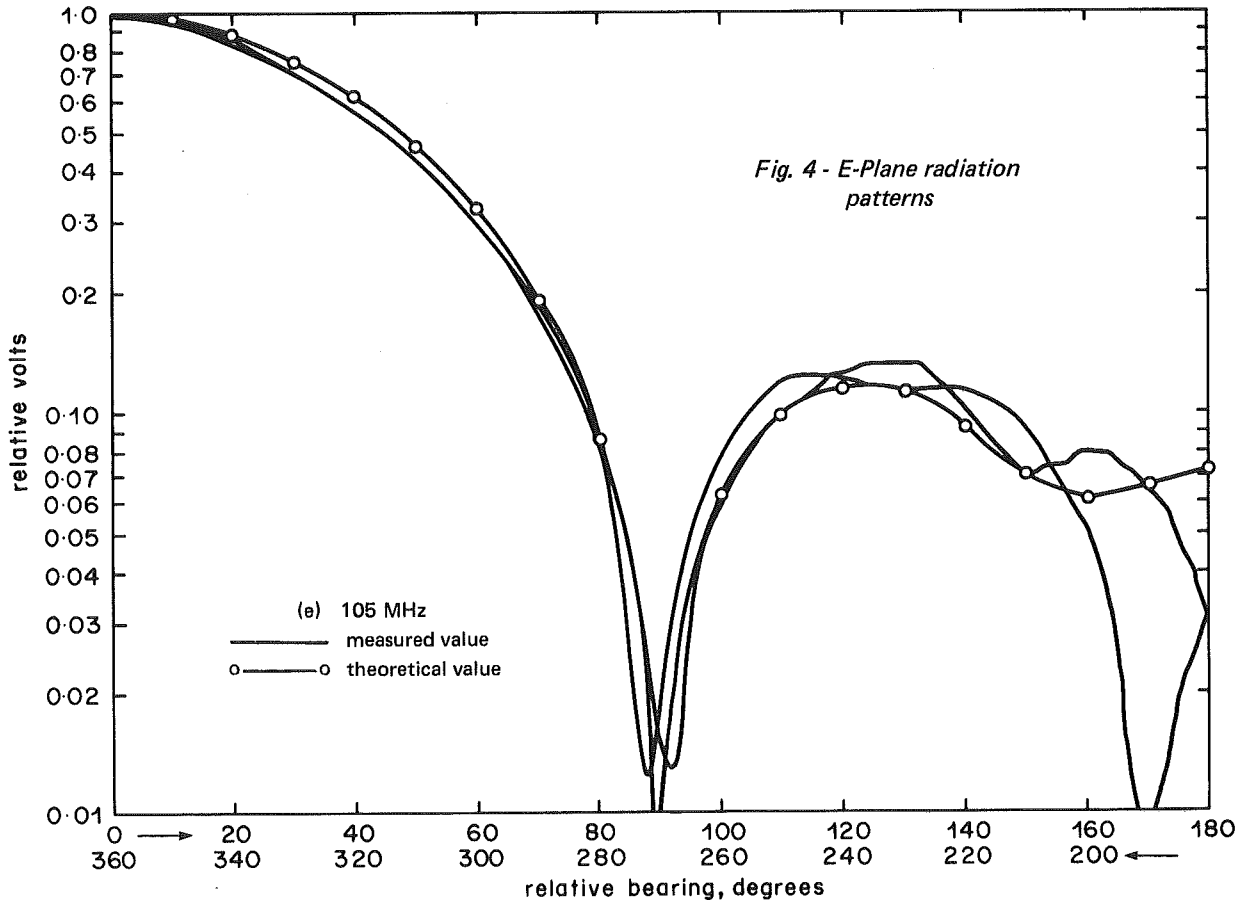

Fig. 4 - E-Plane radiation patterns

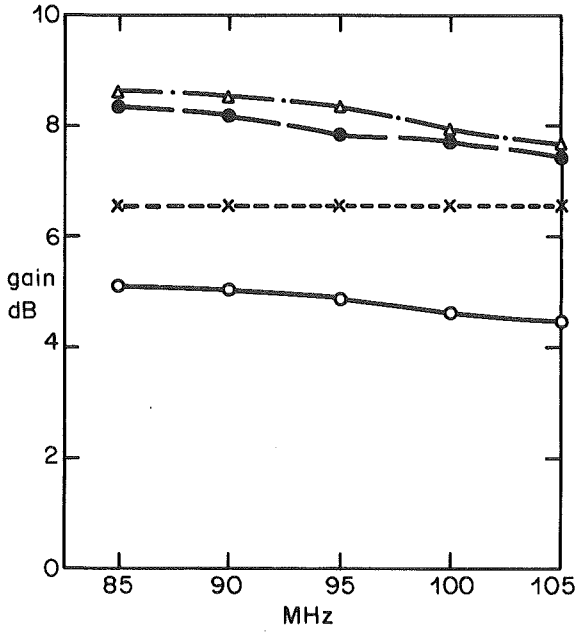

Fig. 5 - Power gain relative to a λ/2 dipole

o——o single array
x- - - -x parallel pair of arrays 0·25λ apart
△—·—△ parallel pair of arrays 0·75λ apart
●— —● parallel pair of arrays 1·0λ apart

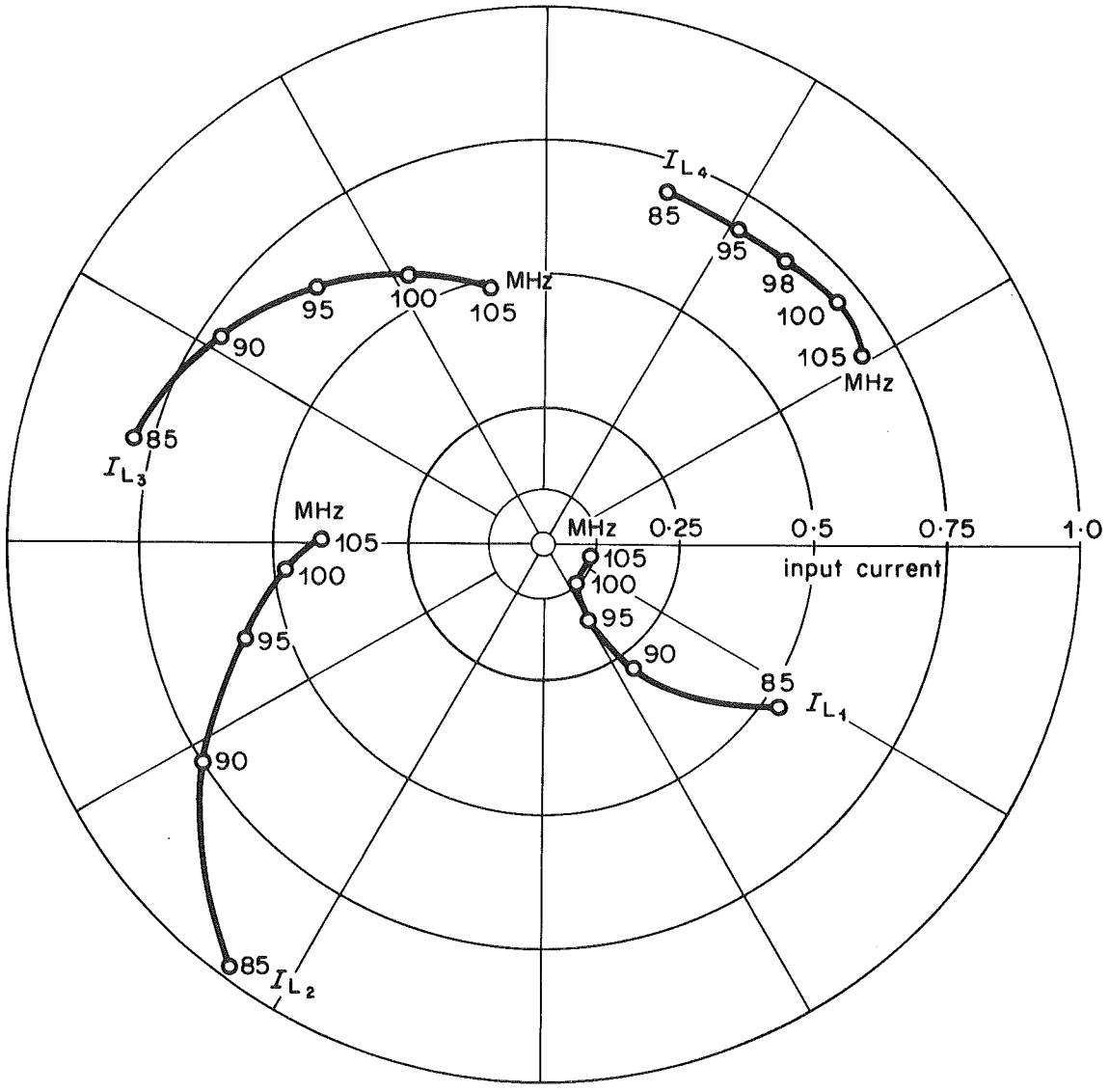

Fig. 6 - Element drive-point currents

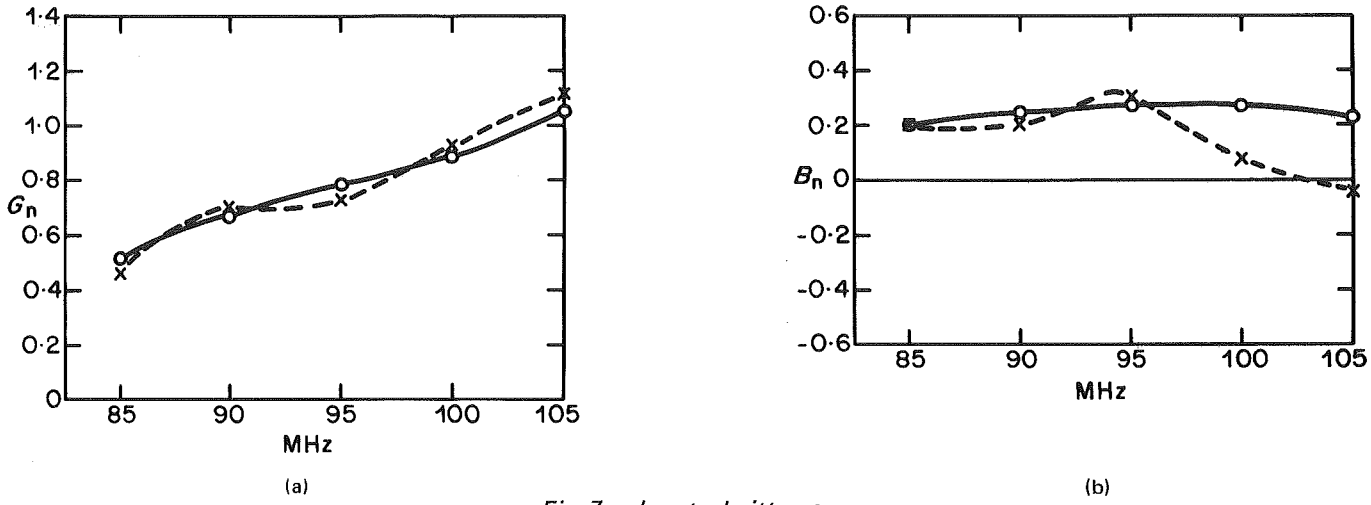

Fig. 7 - Input admittance

(a) normalised conductance (b) normalised susceptance
Values normalised to 20mS
o——o theoretical value x- - - - -x measured value

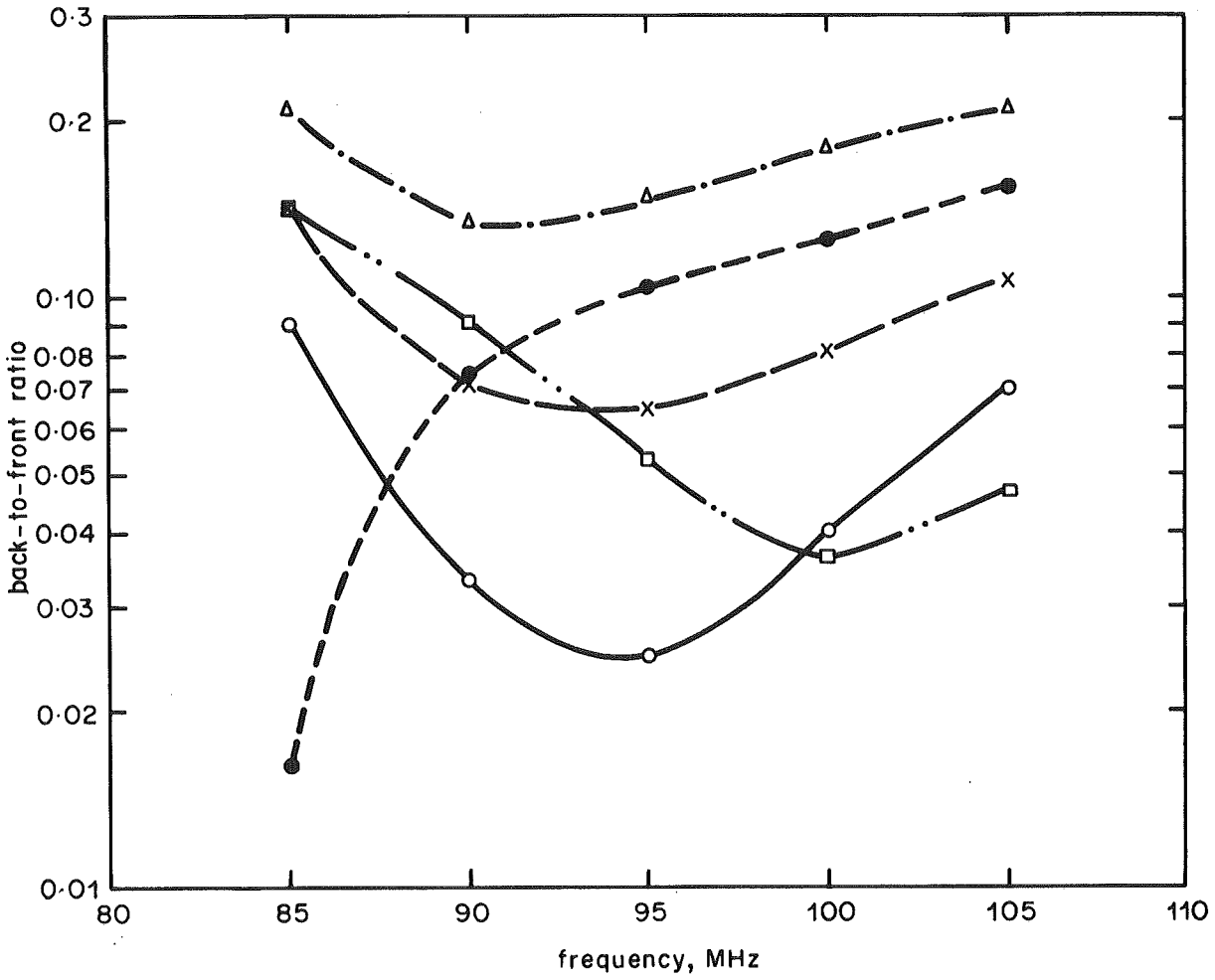

Fig. 8 - Back-to-front ratios of a single array and stacked pairs of arrays

o——o single array x- - - - -x parallel pair of arrays 0·25λ apart
△— · —△ parallel pair of arrays 0·75λ apart ●- - - - -● parallel pair of arrays 1·0λ apart
□— · · —□ parallel pair of arrays 1·5λ apart

7. Conclusions

A four element end-fire array of dipoles has been developed with the aid of a computer program to operate as a transmitting or receiving aerial in the frequency range 88 to 100 MHz. Scale model measurements have been made to check the calculated performance, and the radiation patterns show good agreement. The theoretical and measured input admittances are also in good agreement except for a slight departure at the higher frequencies, but it is anticipated that closer agreement will be obtained with measurements performed on a full-size aerial.

It is foreseen that this array will be needed as a replacement for existing Yagi arrays at Band II Relay Stations should the operational band be extended to 100 MHz in the future. The design gives an acceptable performance over the whole of the 88 to 100 MHz range. It should satisfy most requirements for this type of aerial in applications to horizontally polarised Band II transmitting arrays at relay stations.

8. References

1. CARREL, R. 1961. The design of log-periodic dipole antennas. IRE Int. Conv. Rec. 1961, 6, pp. 61-75.

2. TERMAN, F.E. 1947. Radio Engineering. New York and London, McGraw-Hill Book Company, 1947.

3. BARZILAI, G. 1948. Mutual impedance of parallel aerials. Wireless Eng. 1948, November, 25, pp. 343-352.

APPENDIX 1

Theoretical solution of the array problem

The method used in this report has been described elsewhere[1] but has been included for easy reference.

The array can be represented by networks A and B shown in Fig. 9. Network A consists of the parallel radiating elements of the array, the element drive voltages and currents can be expressed in terms of the self and mutual impedances such that:

$$\mathbf{V_A} = \mathbf{Z_A}\ \mathbf{I_A} \text{ where } \mathbf{Z_A} \text{ is a } Z \text{ matrix;}$$

$\mathbf{V_A}$ and $\mathbf{T_A}$ are column vectors.

They can also be represented by self and mutual admittances

$$\mathbf{I_A} = \mathbf{Y_A}\ \mathbf{V_A} \text{ where } \mathbf{Y_A} \text{ is a } Y \text{ matrix} = \mathbf{Z_A}^{-1}$$

Block B represents the feeder network. The input similarly expressed as $\mathbf{I_B} = \mathbf{Y_B}\ \mathbf{V_B}$.

In Fig. 9 the n^{th} node input current $I_{in(n)} = I_{A(n)} + I_{B(n)}$

For the whole network

$$\mathbf{I_{in}} = \mathbf{Y_A}\ \mathbf{V_A} + \mathbf{Y_B}\ \mathbf{V_B} \tag{1}$$

where $\mathbf{I_{in}}$ is a column matrix.

but

$$V_A = V_B = V$$

$$\therefore\ \mathbf{I_{in}} = [\mathbf{Y_A} + \mathbf{Y_B}]\ \mathbf{V}$$

$$= (\mathbf{Y_A}\ \mathbf{Z_A} + \mathbf{Y_B}\ \mathbf{Z_A})\ \mathbf{I_A}$$

$$\mathbf{Y_A}\ \mathbf{Z_A} = \mathbf{U} \text{ where } \mathbf{U} \text{ is a unit matrix}$$

therefore

$$\mathbf{I_{in}} = (\mathbf{U} + \mathbf{Y_B}\ \mathbf{Z_A})\ \mathbf{I_A}$$

Say

$$\mathbf{I_{in}} = \mathbf{W}\ \mathbf{I_A} \tag{2}$$

The $\mathbf{Z_A}$ matrix for the array is derived from the network equations[2]

$$V_1 = I_1 Z_{11} + I_2 Z_{12} + I_3 Z_{13} \cdots I_n Z_{1n}$$

$$V_2 = I_1 Z_{21} + I_2 Z_{22} + I_3 Z_{23} \cdots$$

$$V_n = I_1 Z_{n1} + \qquad\qquad \cdots I_n Z_{nn}$$

Z_{rr} = self impedance of element r

Z_{sr} = mutual impedance between elements s and r

$$\begin{pmatrix} V_1 \\ V_2 \\ \cdot \\ \cdot \\ \cdot \\ V_n \end{pmatrix} = \begin{pmatrix} Z_{11} & Z_{12} & Z_{13} & \cdot & \cdot & \cdot \\ Z_{21} & Z_{22} & Z_{23} & \cdot & \cdot & \cdot \\ & & \cdot & & & \\ & & \cdot & & & \\ & & \cdot & & & \\ & & \cdot & \cdot & \cdot & Z_{nn} \end{pmatrix} \begin{pmatrix} I_1 \\ I_2 \\ \cdot \\ \cdot \\ \cdot \\ I_n \end{pmatrix}$$

The feeder network Y matrix is

$$\begin{pmatrix} I_1 \\ I_2 \\ I_3 \\ \cdot \\ \cdot \\ \cdot \\ I_n \end{pmatrix} = \begin{pmatrix} Y_{11} & -Y_{12} & 0 & 0 & 0 & \cdot & \cdot \\ -Y_{21} & Y_{22} & -Y_{23} & 0 & 0 & \cdot & \cdot \\ 0 & -Y_{32} & Y_{33} & -Y_{34} & 0 & \cdot & \cdot \\ \cdot & \cdot & \cdot & \cdot & \cdot & \cdot & \cdot \\ \cdot & \cdot & \cdot & \cdot & \cdot & \cdot & \cdot \\ \cdot & \cdot & \cdot & \cdot & \cdot & \cdot & \cdot \\ \cdot & \cdot & \cdot & \cdot & 0 & -Y_{n,(n-1)} & Y_{n,n} \end{pmatrix} \begin{pmatrix} V_n \\ V_2 \\ V_3 \\ \cdot \\ \cdot \\ \cdot \\ V_n \end{pmatrix} \qquad (3)$$

The zero terms arise because the line interconnection is between adjacent nodes only. If alternate output ports are reversed, as in the alternate feeder system, the signs of all coefficients are positive.

The coefficients of the matrix can be obtained by assuming that one pair of input terminals is driven with a voltage V and that all other pairs of terminals are short circuited. For port 2 say, matrix 3 reduces to give the following values:

$$\begin{aligned} I_1 &= -Y_{12}\, V_2 \\ I_2 &= Y_{22}\, V_2 \\ I_3 &= -Y_{32}\, V_2 \\ I_4 &= 0 \\ I_5 &= 0 \\ I_n &= 0 \end{aligned}$$

The admittance values are obtained directly from well known transmission line equations which give:

$$\begin{aligned} Y_{12} &= -\mathrm{j}Y_o \operatorname{cosec} \beta L_{12} \\ Y_{22} &= -\mathrm{j}Y_o \,(\cot \beta L_{21} + \cot \beta L_{23}) \\ Y_{32} &= -\mathrm{j}Y_o \operatorname{cosec} \beta L_{32} \end{aligned}$$

This process is applied at all ports and the Y matrix becomes:

$$-\mathrm{j}Y_o \begin{pmatrix} \cot \beta L_{12} & -\operatorname{cosec} \beta L_{12} & 0 & 0 \\ -\operatorname{cosec} \beta L_{21} & \cot \beta L_{21} + \cot \beta L_{23} & -\operatorname{cosec} \beta L_{23} & 0 \\ 0 & -\operatorname{cosec} \beta L_{32} & \cot \beta L_{32} + \cot \beta L_{34} & -\operatorname{cosec} \beta L_{34} \\ 0 & 0 & & \text{etc} \end{pmatrix} \qquad (4)$$

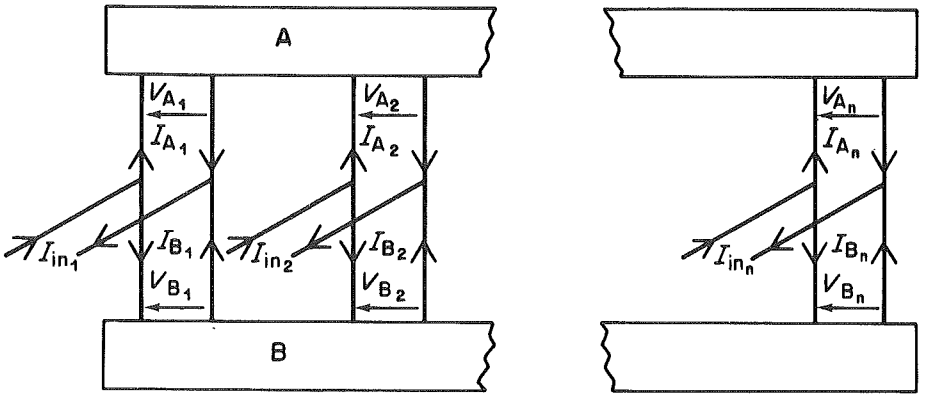

Fig. 9 - Schematic arrangement of array networks

Selection of a single pair of input terminals to the array is achieved by setting the appropriate term in $\mathbf{I}_{in}$ to one ampere and all other values to zero. The solution for element currents is then performed by matrix multiplication and addition to obtain W in equation (2) and inversion of W so that $\mathbf{W}^{-1}\,\mathbf{I}_{in} = \mathbf{I}_A$, where $\mathbf{W}^{-1}$ is the inverse of **W**.

Having established the element currents, the element drive point voltages can be determined from $\mathbf{V}_A = \mathbf{Z}_A\,\mathbf{I}_A$. At the array input terminals, say terminals m, the input current has been set to 1 and the input impedance is therefore given by $Z_m = V_m = (Z_{m1}\ Z_{m2}\ Z_{m3} \cdots Z_{mn})\ \mathbf{I}_A$.

The E-plane and H-plane radiation patterns can be calculated from the element current values $\mathbf{I}_A$ and the maximum gain is determined from

$$G = 10 \log_{10} \frac{73{\cdot}0}{\text{Re}\ \mathbf{Z}_m} (P)^2 \text{ dB} \qquad (5)$$

where P is the normalising factor for the H-plane radiation pattern.*

The sequence of operations for calculating the array performance in the computer program is as follows:

1. Determination of self and mutual impedances for radiating elements from integral equations[3] derived by the induced e.m.f. method. An extended form of Simpson's rule is used to perform the numerical integration.

2. Computation of the elements and formation of the feeder network Y matrix.

3. Matrix multiplication, addition and inversion using a UCC library program to give the element current values.

4. Determination of the array input impedance.

5. Calculation of the E-plane and H-plane radiation patterns. These are determined respectively from the following two equations:

$$E_{(H)} = \sum_{1}^{n} I_n \left\{ \frac{\cos(\beta h_n \sin\theta) - \cos(\beta h_n)}{\sin(\beta h_n)\cos\theta} \right\} e^{j\beta d_n \cos\theta}$$

$$E_{(E)} = \sum_{1}^{n} I_n \left\{ \frac{1 - \cos(\beta h_n)}{\sin(\beta h_n)} \right\} e^{j\beta d_n \cos\phi}$$

the co-ordinate system used is shown in Fig. 10, h_n is the half length of the n^{th} element.

6. Determination of array gain using equation (5).

* $\mathbf{I}_A$ corresponds to unit input current to the array. P is the ratio of far field from the array for unit input current to the far field from a half-wave dipole, at the same distance, for unit input current. The array field is calculated from the expressions in item 5.

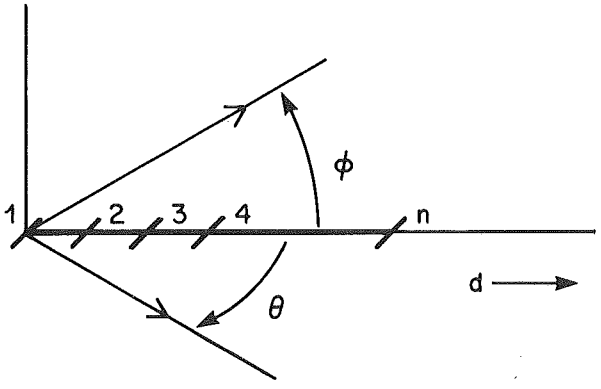

Fig. 10 - Radiation patterns co-ordinate system

APPENDIX II

Improvement of impedance characteristics

An arrangement for improving the impedance match of the array to a 50Ω cable is shown in Fig. 11.

A balanced 100Ω line is used as the interconnecting feeder between elements 1 to 4 and for the short circuit stub as shown in Fig. 2. At element 4, the Z_o of the line is reduced to 75Ω by reducing the separation between conductors and loading the line with polythene dielectric sheet. The feed point for the input cable is at 0·1λ from element 4 along this line (λ corresponds to the electrical wavelength at 94 MHz). A shunt compensating stub is also provided at this point. It consists of a short-circuited stub 0·1λ long formed from the 75Ω Z_o balanced line and an open-circuit coaxial stub with end capacitance tuning. The latter are contained within one conductor of the balanced lines. The theoretical input impedance provided by this arrangement gives a reflection coefficient of less than 5% over the frequency range 87—100 MHz.

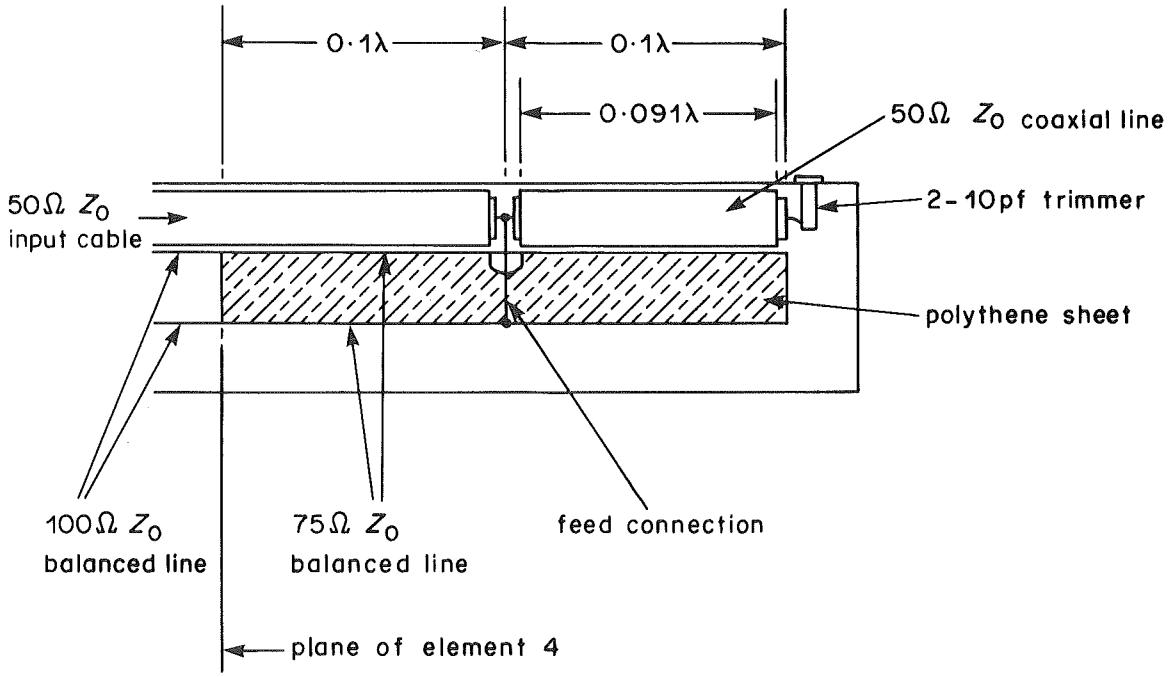

Fig. 11 - Impedance matching arrangement for the array

Printed by BBC RESEARCH DEPARTMENT, Kingswood Warren, Tadworth, Surrey, KT20 6NP